25th IAHR International Symposium on Ice
Trondheim, 23 - 25 November 2020

Fully Dispersive Models for Flexural-Gravity Waves

Evgueni Dinvay[1,2], Henrik Kalisch[2], Emilian I. Parau[3]
[1]*UFR mathématiques, Université de Rennes 1, 35042 Rennes CEDEX, France*
evgueni.dinvay@uib.no
[2]*University of Bergen, Department of Mathematics, PO Box 7800, 5020 Bergen, Norway*
henrik.kalisch@uib.no
[3]*University of East Anglia, School of Mathematics, Norwich, NR4 7TJ, UK*
E.Parau@uea.ac.uk

We propose a mathematical model which describes the time-dependent response to of a floating ice sheet to a load moving at an arbitrary, possibly time-dependent velocity. The model is validated using a number of test cases from existing field studies, such as the field campaign of Takizawa at Lake Saroma and the campaign of Wilson at Mille Lacs. Good agreement between the deflectometer records from the field studies and the numerical simulations is observed in most cases.

The model allows for an accurate description of waves across the whole spectrum of wavelengths and also incorporates nonlinearity, forcing and damping. The load can be a point load or have a described weight distribution, moving at a time-dependent velocity. In this respect, the present model is more versatile than existing models for steady waves excited by moving loads.

1. Introduction

Hydro-elastic waves can be found in ice sheets in the arctic regions and on frozen lakes and sounds in the winter season. The study of such waves has a long history going back to the 1950's and was prompted by attempts to use solid ice covers as a means of supporting mechanized transportation (Squire et al., 1988). For example, in cold regions, some winter truck routes are partially on ice-covered lakes, and in some cases air strips have been built on thick ice covers. Indeed as mentioned in (Squire et al., 1988), in some cases, train tracks have been laid on ice.

As many of these enterprises experienced problems resulting in loss equipment, and sometimes even endangering the life of the crews, it became clear that there was a need to improve our understanding of the properties of ice covers such as bearing capacity, resonant behavior, and the susceptibility to crack formation. A number of experimental campaigns were mounted with the goal of understanding the wave response to moving loads on ice covers (Takizawa, 1987), (Takizawa, 1988), (Wilson, 1955). In addition, mathematical models were developed in order to predict the wave response to a moving load (Davys, Hosking and Sneyd, 1985). This purely linear conservative model was later improved by including nonlinearity (Parau and Dias, 2002), (Guyenne and Parau, 2014a, 2014b) and various forms of damping or visco-elasticity (Hosking, Sneyd and Waugh, 1988), (Wang, Hosking and Milinazzo, 2004).

In the current contribution, we use a fully dispersive model equation developed in (Dinvay, Kalisch and Parau, 2019a, 2019b) which is able to give more detailed information on the waves excited by a moving load than many previous works. The derivation is based on an idea due to G.B. Whitham (Whitham, 1967) to couple fully dispersive models with weakly linear terms, which has recently been extended to systems of equations (Aceves-Sanchez, Minzoni, and Panayotaros, 2013), (Carter, 2018), (Dinvay, Dutykh and Kalisch, 2019), (Moldabayev, Kalisch, Dutykh, 2015). Using this new model in connection with a split-step method for numerical discretization, we are able to study the time-dependent development of flexural-gravity waves. The versatility of the model system allows the study of a wide range of situations including the motion of a combination of point loads, or indeed loads of arbitrary shape and time-dependent velocity.

A point of departure for the linear study of flexural-gravity waves is the dispersion relation for small-amplitude waves. This relation is given by

$$c^2(\xi) = \frac{g/\xi + D\xi^3/\rho}{\coth \xi H + h\xi\rho_I/\rho} \tag{1.1}$$

where H is the depth of the undisturbed fluid, h is the thickness of the elastic cover, ρ is the fluid density, ρ_I is the density of the elastic cover, and D is the flexural rigidity of the elastic material. In stating the relation (2.1), the assumption is made that the wavelength is greater than the thickness of the ice sheet. This assumption is generally reasonable. On the other hand, for very long waves the above relation may be approximated by

$$c^2 = \frac{g}{\xi}[1 + \xi^4 D/g\rho\,]\tanh \xi H \tag{1.2}$$

which is used in Takizawa (1987) and many other works. Figure 1 shows the two

dispersion relations (1.1) and (1.2) for the parameter sets corresponding to the field experiments reported in (Takizawa, 1987,1988) and (Wilson, 1955). In the following we shall look at the derivation of the hydro-elastic equations, then state the weakly nonlinear approximation, and finally present numerical simulations of the field experiments of Takizawa and Wilson.

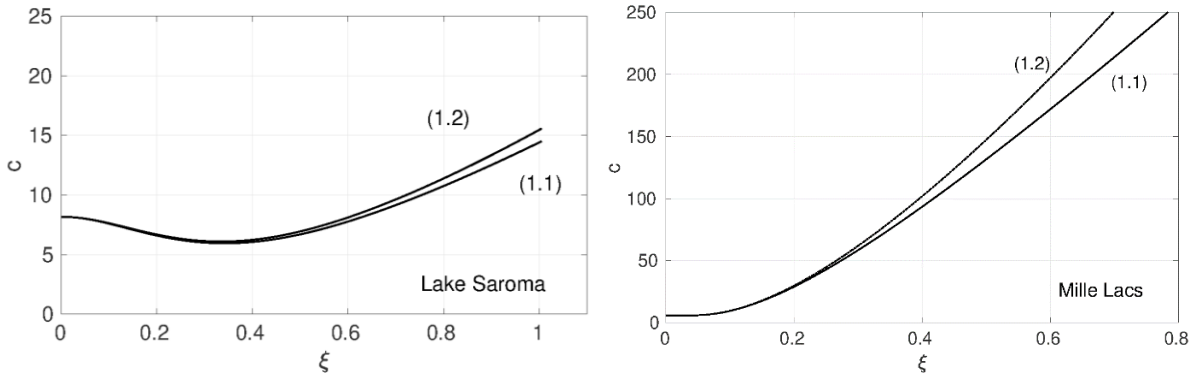

Figure 1. Dispersion of flexural gravity waves on Lake Saroma (Takizawa, 1987) and on Mille Lacs (Wilson, 1955).

2. The hydro-elastic system

We consider irrotational motion of an inviscid and incompressible fluid of undisturbed mean depth H, and with gravity g acting in the negative z-direction. The fluid is covered by an elastic solid described by the Kirchhoff–Love plate theory (cf. Squire, Hosking, Kerr & Langhorne (1988)). The flow of the underlying liquid is described by the velocity potential $\Phi(x, z, t)$ and by the fluid surface elevation $\eta(x,t)$ that coincides with the vertical deformation of the underside of the elastic cover. The surface z = 0 corresponds to the fluid-solid interface at rest. The fluid flow is describe by the Euler equations, i.e. the Laplace equation

$$\Phi_{xx} + \Phi_{zz} = 0 \qquad \text{for } x \in \boldsymbol{R}, \qquad -H < z < \eta(x,t) \tag{2.1}$$

the Neumann boundary condition at the bottom

$$\Phi_z = 0 \qquad \text{at } z = -H, \tag{2.2}$$

the kinematic condition at the interface between the cover and the liquid

$$\eta_t + \Phi_x \eta_x - \Phi_z = 0 \qquad \text{for } x \in \boldsymbol{R}, \qquad z = \eta(x,t) \tag{2.3}$$

and the dynamic boundary condition

$$\Phi_t + \frac{1}{2}|\nabla\Phi|^2 + g\eta + \frac{p}{\rho} = C_B \qquad \text{for } x \in \boldsymbol{R}, \qquad z = \eta(x,t). \tag{2.4}$$

Here C_B is the Bernoulli constant which will be specified later. The presence of the elastic solid is described via the pressure at the boundary. To model the elastic medium we regard a new

coordinate system shifted up along the z-axis, so that the line z = 0 coincides with z = h/2, where h is the ice thickness. Thus at rest, the line z = 0 coincides with the the center line of the elastic plate. For ease of reading, the developments in this section are only given for the two-dimensional case. The three dimensional case can be treated analogously. Assuming small deformations in the horizontal and vertical directions respectively, one may consider the following material motion equations

$$\partial_x \sigma_{11} + \partial_z \sigma_{12} = \rho_I \partial_t^2 u_1 \tag{2.5}$$

$$\partial_x \sigma_{21} + \partial_z \sigma_{22} - \rho_I g = \rho_I \partial_t^2 u_2 \tag{2.6}$$

This system represents Newton's second law connecting the divergence of the stress tensor on the left hand side and the acceleration of particles on the right simplified due to smallness of the deformation. The plate density is constant. The stress tensor is symmetric, which means there are no volume or surface moments. As is common in hydro-elastic problems, we combine nonlinear equations for the fluid motion with linear elastic equations for the solid. This choice can be justified by noticing that liquid motions are of a different order of magnitude than deformations of the elastic solid cover. The equations are completed by adding the relation

$$u_1 = -z\partial_x u_2 \tag{2.7}$$

with u_2 not depending on z and

$$\sigma_{11} = \frac{E}{1-\nu^2}\partial_x u_1 \tag{2.8}$$

Here E is Young's modulus and ν is Poisson's ratio of the solid. Equation (2.7) is a consequence of the first Kirchhoff hypothesis stating that straight lines normal to the mid-surface remain normal and straight after deformation. It also assumes that the thickness does not change during deformation. Equation (2.8) is a Hooke relation modified by the second Kirchhoff hypothesis stating that normal stresses to surfaces parallel to the center surface are smaller than other stresses. The validity of the last assumptions (2.7)-(2.8) are well justified provided the plate thickness h is small with respect to horizontal scales. That is true since we consider a domain of infinite extent in the horizontal directions. Note that we do not assume anything concerning the relation between the thickness h and the depth H.

With regards to boundary conditions imposed on the elastic plate, we have an inviscid fluid below the plate, which means that the shear stress at the lower boundary is zero and the normal stress is due to the fluid pressure p. The top of the elastic plate is free, except for an imposed pressure P which can be used to model a moving load. Summing up, we have

$$\sigma_{22} = -P(x,t) \text{ on } z = h/2,$$
$$\sigma_{22} = -p(x,t) \text{ on } z = -h/2,$$
$$\sigma_{12} = \sigma_{21} = 0 \text{ on } z = h/2 \text{ and } z = -h/2.$$

An agreement is made here that the liquid pushes the plate up and the load pushes it down. In a real situation this will mean that the pressure P is positive, in case of a heavy truck for example. However, mathematically, negative values of the imposed load P are also allowed.

Following Squire, Hosking, Kerr & Langhorne (1988), a standard procedure of averaging the expressions (2.5)-(2.6) is now applied. Introduce a transverse force

$$Q_1 = \int_{-h/2}^{h/2} \sigma_{12}\, dz.$$

Integrating both parts of (2.6) over z one obtains

$$\partial_x Q_1 + \sigma_{22}|_{z=-h/2}^{z=h/2} - \rho_I g h = \rho_I h \partial_t^2 u_2.$$

Substituting (2.7)-(2.8) in the first equation (2.5), then multiplying by −z and integrating over z one arrives at

$$\frac{Eh^3}{12(1-\nu^2)}\partial_x^3 u_2 + Q_1 - z\sigma_{12}|_{z=-\frac{h}{2}}^{z=\frac{h}{2}} = \frac{\rho_I h^3}{12}\partial_t^2 \partial_x u_2.$$

These two equations together with the boundary conditions yield the relation

$$D\partial_x^4 u_2 - \frac{\rho_I h^3}{12}\partial_t^2 \partial_x^2 u_2 + \rho_I h \partial_t^2 u_2 + \rho_I g h + P - p = 0$$

where $D = Eh^3/12(1-\nu^2)$ is the flexural rigidity. This is a well known equation describing the deflection $u_2(x,t)$ of a beam. The second term in the equation which is due to horizontal acceleration of media particles is usually neglected, but in the present analysis, this term will actually be important.

The last step in the modelling of the elastic cover is to take into account energy dissipation. We assume a damping force proportional to the vertical velocity, which results in the addition of a damping term to the left part of equation (2.6). Repeating the above averaging procedure in the presence of damping leads to

$$D\partial_x^4 u_2 - \frac{\rho_I h^3}{12}\partial_t^2 \partial_x^2 u_2 + \rho_I h \partial_t^2 u_2 + b\partial_t u_2 + \rho_I g h + P - p = 0 \qquad (2.9)$$

which is our main ice deflection model that we need to combine with Equations (2.1)-(2.4). As stated above, the vertical deformation does not depend on variable z. Moreover, we do not allow for cavitation, so that the underlying fluid is always in contact with the elastic plate. Therefore the curves $z = u_2(x, t) - h/2$ and $z = \eta(x, t)$ coincide. If we now choose the Bernoulli constant $C_B = g\,\rho_I h/\rho$, then the last equation (2.9) together with (2.4) can be written in terms of the hydro-elastic parameter $\kappa = D/(\rho g)$ as

$$\kappa g \partial_x^4 \eta - \frac{\rho_I h^3}{12\rho}\partial_t^2 \partial_x^2 \eta + \frac{\rho_I h}{\rho}\partial_t^2 \eta + \frac{b}{\rho}\partial_t \eta + g\eta + \Phi_t + \frac{1}{2}|\nabla\Phi|^2 + \frac{P}{\rho} = 0. \qquad (2.10)$$

This equation holds on the interface $z = \eta(x, t)$. Note that both the horizontal acceleration of the solid media particles and the nonlinear hydrodynamical effects are taken into account here. The load P is taken as a distributed pressure

$$P(x,t) = \rho f(x - x_0 - X(t)) \qquad (2.11)$$

propagating down the x-axis. The hydro-elastic system is given thus by the Laplace equation (2.1), with the boundary conditions (2.2), (2.3) and (2.10).

3. Weakly nonlinear models and simulations

Using an analysis such as presented in (Dinvay, Kalisch and Parau, 2019a, 2019b), a fully dispersive weakly nonlinear system can be found. The system has the form

$$\eta_t = -\frac{\tanh HD}{D} u_x - \partial_x(\eta u) \tag{3.1}$$

$$u_t = -g\frac{1+\kappa\partial_x^4}{K}\eta_x - \frac{b}{\rho}\frac{G_0}{K}u - \frac{\rho_I g h}{2\rho}\partial_x^3\eta^2 + \frac{b}{\rho}\partial_x^2(\eta u) - uu_x - \Gamma_x, \tag{3.2}$$

where $D = -i\partial_x$, $G_0 = D\tanh(HD)$ and $K = 1 + \rho_I h/\rho\, D\tanh(HD)$ are Fourier multiplier operators and Γ_x represents the forcing by the moving load. In the following, we present results of simulations of this system. In order to approximate solutions, a spectral method coupled with a second-order split-step scheme is utilized. Details of this process can be found in (Dinvay, Kalisch and Parau, 2019a).

First, we consider the field experiments of Takizawa. In this case, the ice thickness was 0.16m, the depth was 6.8m, and the load was a skidoo weighing 235kg. The skidoo was driven on a test track at various sub and supercritical speeds. Figure 2 shows the results of measurements taken at a fixed measurement point along the test track. The time series obtained by Takizawa are digitized and compared with numerical simulations of the model (3.1), (3.2). The comparison is favorable except for the near-critical speed 5.5 m/s.

In Figure 3, similar comparisons are made with the data obtained during the field campaign of Wilson on Mille Lacs (Wilson, 1955). In this case, the ice layer was 61cm thick, and the water depth was 3.26m. Two trucks were driven over the lake simultaneously. Several runs with varying separation are shown in Figure 3, and the agreement between the measurements and the simulations is very good.

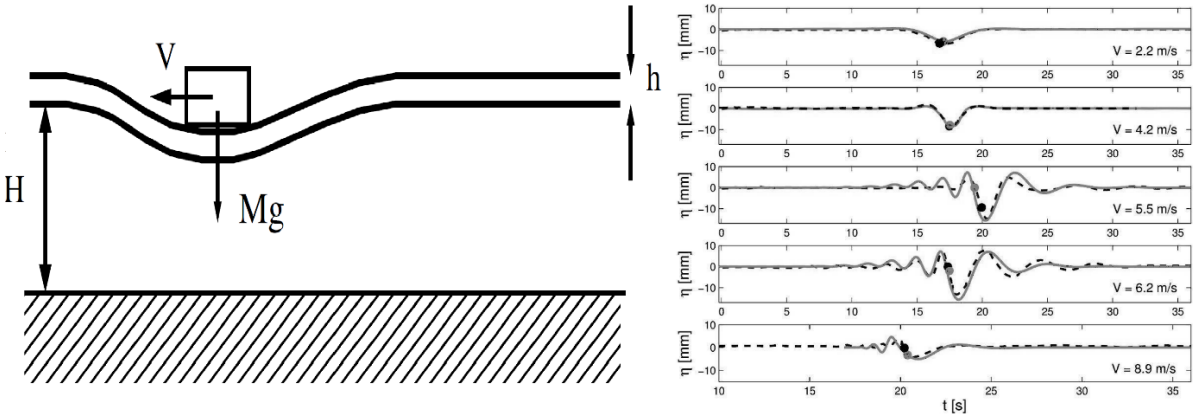

Figure 2. Single point load used by Takizawa during experiments on Lake Saroma. The right panel shows comparison between time series measured at a fixed measurement location, and

a time series taken from a simulation of the experiment using the parameters documented in (Takizawa, 1987).

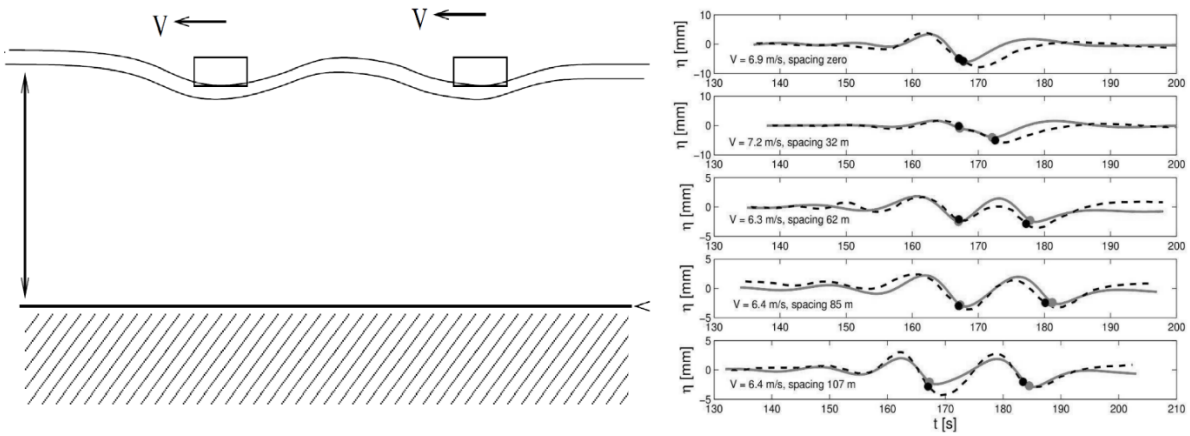

Figure 3. Double load used by Wilson during experiments on Mille Lacs. The right panel shows comparison between time series measured at a fixed measurement location, and a time series taken from a simulation of the experiment using the parameters documented in (Wilson, 1955).

Acknowledgments
This research was supported by the Research Council of Norway through grant no. 239033/F20 and by the EPSRC under grant EP/J019305/1. The authors would like to thank two anonymous reviewers for valuable comments.

References

Aceves-Sanchez, P., Minzoni, A.A. and Panayotaros, P., 2013. Numerical study of a nonlocal model for water-waves with variable depth. Wave Motion 50, 80–93.

Carter, J.D.. 2018. Bidirectional Whitham equations as models of waves on shallow water. Wave Motion 82, 51–61.

Davys, J.W., Hosking, R.J. and Sneyd, A.D., 1985. Waves due to a steadily moving source on a floating ice plate. J. Fluid Mech. 158, 269–287.

Dinvay, E., Dutykh, D. and Kalisch, H., 2019. A comparative study of bi-directional Whitham systems. Appl. Numer. Maths 141, 248–262.

Dinvay, E., Kalisch, H and Parau, E.I., 2019a. Fully dispersive models for moving loads on ice sheets. J. Fluid Mech. 867, 122-149.

Dinvay, E., Kalisch, H and Parau, E.I., 2019b. The Whitham equation for hydroelastic waves. Appl. Ocean Research 89, 202-210.

Guyenne, P. and Parau, E.I., 2014a., Finite-depth effects on solitary waves in a floating ice-sheet. J. Fluids Struct. 49, 242–262.

Guyenne, P. and Parau, E.I., 2014b., Forced and unforced flexural-gravity solitary waves. In Proc. IUTAM, vol. 11, pp. 44–57. Elsevier.

Hosking, R.J., Sneyd, A.D. and Waugh, D.W. 1988., Viscoelastic response of a floating ice ice plate to a steadily moving load. J. Fluid Mech. 196, 409–430.

Marko, J.R. 2003. Observations and analyses of an intense waves-in-ice event in the Sea of Okhotsk. J. Geophys. Res. 108 (C9), 3296.

Milinazzo, F., Shinbrot, M. and Evans, N.W., 1995. A mathematical analysis of the steady response of floating ice to the uniform motion of a rectangular load. J. Fluid Mech. 287,173-197.

Moldabayev, D., Kalisch, H. and Dutykh, D., 2015. The Whitham equation as a model for surface water waves. Physica D 309, 99–107.

Parau, E.I. and Dias, F., 2002. Nonlinear effects in the response of a floating ice plate to a moving load. J. Fluid Mech. 460, 281–305.

Squire, V.A., Hosking, R.J., Kerr, A.D. and Langhorne, P.J., 1988. Moving Loads on Ice Plates. Kluwer.

Takizawa, T. 1987 Field studies on response of a floating sea ice sheet to a steadily moving load. Contrib. Inst. Low Temp. Sci. A 36, 31–76.

Takizawa, T., 1988. Response of a floating sea ice sheet to a steadily moving load. J. Geophys. Res. 93, 5100–5112.

Wang, K., Hosking, R.J. and Milinazzo, F., 2004, Time-dependent response of a floating viscoelastic plate to an impulsively started moving load. J. Fluid Mech. 521, 295–317.

Whitham, G.B., 1967. Variational methods and applications to water waves. Proc. R. Soc. Lond. A 299, 6–25.

Wilson, J.T., 1955. Coupling between moving loads and flexural waves in floating ice sheets. US Army SIPRE Report 34.